

# Robust half-metallicity and metamagnetism in $\text{Fe}_x\text{Co}_{1-x}\text{S}_2$

I.I. Mazin

Code 6391, Naval Research Laboratory, Washington, DC 20375

(January 19, 2000)

The  $\text{Fe}_x\text{Co}_{1-x}\text{S}_2$  system is predicted, on the basis of density functional calculations, to be a half metal for a large range of concentrations. Unlike most known half metals, the half metallicity in this system should be very stable with respect to crystallographic disorder and other types of defects. The endmember of the series,  $\text{CoS}_2$ , is not a half metal, but exhibits interesting and unusual magnetic properties which can, however, be reasonably well understood within the density functional theory, particularly with the help of the extended Stoner model. Calculations suggest strong electron-phonon and electron-magnon coupling in the system, and probably a bad metal behavior at high temperatures.

*God made the integers, all else is the work of man*  
(L. Kronecker).

Half metals (HM), materials that are metals in one spin channel and insulators in the other, are attracting substantial interest recently, mostly because of potential application in spintronics devices, *e.g.*, spin valves [1]. Unfortunately, although a few dozen various materials have been predicted to be HM on the basis of band structure calculations, there are hardly any that have been convincingly confirmed to be such by an experiment. A possible exception is  $\text{CrO}_2$  where a spin polarization of up to 90% was measured by the Andreev reflection technique [2] (in some other materials there is indirect evidence such as integer magnetic moment or optical spectra consistent with half-metallic bands). The usual explanation of such a discrepancy between the theory and the experiment is that half-metallicity in these materials is very sensitive to crystallographic disorder and stoichiometry (see, *e.g.*, Ref. [3]). Indeed, no materials have been predicted to be HM in a wide range of concentrations of the constituents, and insensitive to disorder.

In this Letter I point out one such material. Namely, I show that the pyrite alloys  $\text{Fe}_{1-x}\text{Co}_x\text{S}_2$  are HM for the most of the concentration range ( $0.1 \lesssim x \lesssim 0.9$ ), and not sensitive to ordering of Fe and Co in the metal sublattice. On the other hand, at  $x \gtrsim 1$  [4], calculations predict magnetic collapse under pressure, and a metamagnetic behavior just before the collapse. Both half metallicity and metamagnetism can be explained by competition between the kinetic (band) energy, and the Stoner (Hund) interaction.

Experimentally, the system of pyrite solid solutions,  $(\text{Fe}, \text{Co}, \text{Ni}, \text{Cu})(\text{S}, \text{Se})_2$ , is amazingly rich.  $\text{FeS}_2$  is a non-magnetic semiconductor, in agreement with the band structure calculations [5,6]. With as little as 0.1% Co, by some data [7], it becomes a ferromagnetic metal, and remains ferromagnetic all the way through  $\text{CoS}_2$ , and further on until approximately  $\text{Co}_{0.9}\text{Ni}_{0.1}\text{S}_2$ . It was noted that the magnetic moment,  $M$ , per Co atom in  $\text{Fe}_{1-x}\text{Co}_x\text{S}_2$  solid solutions stays close to  $1 \mu_B$  in an extremely wide range from  $x \approx 0.1 - 0.2$  to  $x = 0.9 - 0.95$ . To the best of my knowledge, no explanation of this fact

has been suggested till now. At larger  $x$ ,  $M$  decreases to  $\approx 0.85 \mu_B$  [7]. Starting from  $\text{CoS}_2$ , one can also substitute S with Se. The Curie temperature,  $T_C$ , rapidly decreases, and magnetism disappears at Se concentration of 10-12%, while  $M$  decreases only slightly [8]. At larger Se concentrations, the material shows metamagnetic behavior with no sizeable spontaneous magnetization, but with magnetization of  $0.82 - 0.85 \mu_B$  appearing abruptly when applied magnetic field exceeds approximately  $(220x_{\text{Se}} - 25)$  tesla. A very similar behavior was observed in pure  $\text{CoS}_2$  under pressure [8], suggesting that the magnetic effect of Se is just the density of states (DOS) reduction.

As shown below, all these effects are reproduced by the standard local spin density (LSD) calculations, and find their explanation within the extended Stoner model (ESM) [9]. Further substitution of Co by Ni leads to a Mott-Hubbard transition into an antiferromagnetic state, which is, in contrast to the system considered here, poorly described by the LSD. Further doping by Cu leads to a superconductivity, presumably due to high-energy sulfur vibrons [10].

To understand the behavior of the  $\text{Fe}_{1-x}\text{Co}_x\text{S}_2$  system, I performed several series of density functional LSD calculations: First, virtual crystal approximation (VCA) was used in conjunction with the Linear Muffin Tin Orbital (LMTO) method [11]. Then, I did several calculations using rhombohedral supercells of 4 or 8 formula units. Finally, I checked the results against more accurate full-potential linear augmented plane wave calculations [12] for pure  $\text{CoS}_2$ ,  $\text{FeCo}_3\text{S}_8$ , and  $(\text{Fe}_{0.25}\text{Co}_{0.75})\text{S}_2$  in VCA. The results were consistent with the LMTO calculations. All calculations were performed in the experimental crystal structure of  $\text{CoS}_2$ . In reality, the S-S bond in  $\text{FeS}_2$  is 4% longer. The effect on the band structure is not negligible, particularly near the bottom of the conductivity band [13]. However, the difference is not important for the purpose of the current Letter, namely the half metallicity of  $\text{Fe}_{1-x}\text{Co}_x\text{S}_2$  alloys, and understanding the basic physics of its magnetic phase diagram. The resulting magnetic moments are shown in Fig.1. In good agreement with the experiment, the magnetic moment per Co

is exactly  $1 \mu_B$  for the Co concentrations  $0.3 \lesssim x \lesssim 0.9$ . The same holds for the rhombohedral supercell calculations (Fig.1), demonstrating stability of the HM state with respect to crystallographic disorder. I performed calculations for ordered  $\text{Fe}_7\text{CoS}_{16}$ ,  $\text{Fe}_3\text{CoS}_8$ ,  $\text{FeCoS}_4$ , and  $\text{FeCo}_3\text{S}_8$ , and found that already  $\text{Fe}_7\text{CoS}_{16}$  ( $x = 0.125$ ) has magnetic moment of  $1 \mu_B$  per Co. Although the original paper [7] implied that the total magnetic moment resides on Co, this is not true: for instance, in  $\text{Fe}_7\text{CoS}_{16}$  less than 30% of the total magnetization ( $0.45 \mu_B$ ) resides on Co. The nearest neighbor Fe (6 per cell) carry  $\approx 0.15 \mu_B$  each. 8% of the total moment resides on S, about the same relative amount as in  $\text{CoS}_2$  [14]. So, one cannot view the low-doping  $\text{Fe}_{1-x}\text{Co}_x\text{S}_2$  alloys as magnetic Co ions embedded in polarizable  $\text{FeS}_2$  background, as for instance Fe in Pd.

The best way to understand the physics of this alloy is to start with  $\text{FeS}_2$ .  $\text{FeS}_2$  is a nonmagnetic semiconductor with a gap between the  $t_{2g}$  and  $e_g$  states [5,6]. The reason for that is that sulfur forms  $\text{S}_2$  dimers with the  $pp\sigma$  states split into a bonding and an antibonding state. The latter is slightly above the Fe  $e_g$  states and thus empty. The other 5 S  $p$  states are below the Fe  $t_{2g}$  states, hence the occupation of the Fe  $d$  bands is 6, just enough to fill the narrow  $t_{2g}$  band. Magnetizing  $\text{FeS}_2$  would require transfer of electrons from the  $t_{2g}$  into the  $e_g$  band, at an energy cost of the band gap  $\Delta$  per electron. The Stoner parameter  $I$ , which characterizes the gain of Hund energy per one electron transferred from the spin-minority into the spin-majority band, appears to be smaller than  $\Delta \approx 0.75$  eV (For the conductivity band in  $\text{FeS}_2$ , due to hybridization with S,  $I$  is smaller than in pure Fe [15] and is  $\approx 0.55$  eV). However, if we populate the same band structure with  $x \ll 1$  additional electrons per formula unit, we can either distribute them equally between the two spin subband, or place  $x'$  in the spin majority band and  $x'' = x - x'$  in the spin majority band (the total magnetic moment in  $\mu_B$  is then  $M = x' - x''$ ). In the latter case we gain a Hund energy of  $-IM^2/4$ , but we lose kinetic (band structure) energy because some states have only single occupancy and thus more high-energy states have to be occupied. Using effective mass approximation for the conductivity band one can express this kinetic energy loss in terms of concentration  $x$  and magnetic moment per Co  $\beta = M/x$  as  $A(x/2)^{5/3}[(1+\beta)^{5/3} + (1-\beta)^{5/3}]$ , where  $A = \frac{3\hbar^2}{10m^*}(\frac{3}{4\pi V})^{2/3}$ ,  $m^*$  is the effective mass, and  $V$  is the volume per formula unit.

Minimizing the total energy with respect to  $\beta$  gives the equilibrium magnetic moment in ESM:

$$\beta = (5A/3I)[(1+\beta)^{2/3} - (1-\beta)^{2/3}]/(4x)^{1/3}$$

The solution is a universal function  $\beta(Ix^{1/3}/A)$ . Note that  $\beta(z) = 0$  for  $z < 10 \cdot 2^{1/3}/9$ , and  $\beta(z) = 1$  for  $z > 5/3$ . Correspondingly, with doping the material remains paramagnetic until  $x$  reaches  $x_1 = 2(10A/9I)^3$ ,

and then the magnetic moment per Co atom gradually grows until the concentration reaches the  $x_2 = (5A/3I)^3$ . At larger dopings the material remains half-metallic with  $\beta = 1$ . Eventually, DOS starts to deviate from the effective mass model and the polarization  $\beta$  may become smaller than 1 again. One can estimate the critical concentrations  $x_{1,2}$  using the following values, extracted from the band structure calculations for  $\text{FeS}_2$ :  $m^* \approx 0.8$ ,  $I \approx 0.55$  eV. This gives  $x_1 \approx 0.16$  and  $x_2 \approx 0.26$ , in qualitative agreement with the experiment and LSDA calculations (Fig.1).

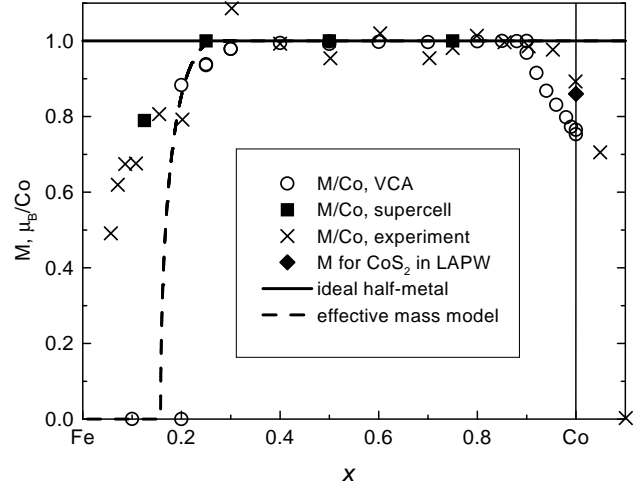


FIG. 1. Experimental and calculated magnetic moment per Co in  $\text{Fe}_{1-x}\text{Co}_x\text{S}_2$  alloys. VCA: virtual crystal approximation, s/cell: supercell calculations, experimental data are from Ref. [7].

This explains the on the first glance unexpected result: in contrast to most known half metals  $\text{Fe}_{1-x}\text{Co}_x\text{S}_2$  remains a HM for a large range of concentrations, is insensitive to crystallographic disorder, and probably not very sensitive to the state of the surface either: the behavior qualitatively described by the universal function  $\beta$  above is determined by the competition of two large energies: The band gap  $\Delta$ , which is a measure of crystal field splitting, and the Stoner factor  $I$ , a measure of the Hund coupling. As long as  $\Delta > I$  and  $x_1 \ll 1$ , a large region of half-metallicity exists. Both conditions are related primarily to the atomic characteristic of constituents and gross features of the crystal structure, and are not sensitive to details.

The same competition between the band energy and the Stoner energy leads to very different magnetic properties in case of stoichiometric  $\text{CoS}_2$ , and of  $\text{CoS}_2$  doped with Ni ( $x > 1$  region in Fig.1). The experimental moment in the stoichiometric compound is  $0.85\text{--}0.9 \mu_B$ , in perfect agreement with full potential LSDA calculations, and in reasonable agreement with LMTO results as well. External pressure, or substituting S by Se, rapidly re-

duces magnetic moment [8]. As shown in Ref. [16], Se doping increases the width of the conductivity band (because the  $\text{Se}_2$  dimer has smaller  $pp\sigma$  splitting than  $\text{S}_2$ , and therefore the Co  $e_g$  states are better aligned with the chalcogen  $pp\sigma^*$  states [13]). Thus Se doping has the same effect as applying pressure. Doping with Ni has similar effect and Ni concentrations of the order of 10% make the system non-magnetic. The large magnetic moment of  $\text{CoS}_2$  suggests that the ferromagnetism in this system is robust and the fact that it disappears so rapidly with pressure and doping seems surprising.

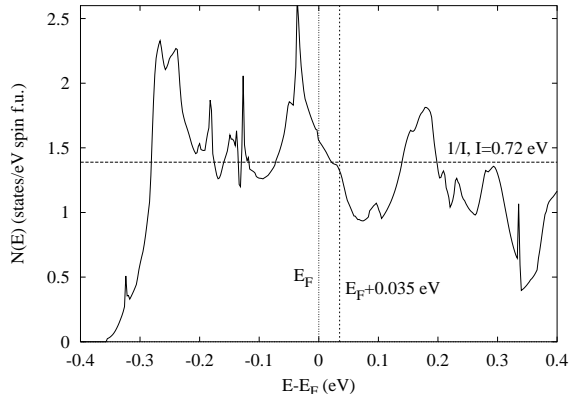


FIG. 2. Density of states for *paramagnetic*  $\text{CoS}_2$ , calculated by LAPW method.  $E - E_F = 0.35$  eV corresponds to  $\text{Co}_{0.9}\text{Ni}_{0.1}\text{S}_2$  in the rigid band approximation.

Since all these effects are reproduced very well by regular LSDA calculations (Fig.1), ESM calculations again provide valuable physical insight. Unlike the parabolic band case considered above, now one has to take into account specific structure of DOS of  $\text{CoS}_2$  (Fig.2). The loss of the one-electron energy can be expressed [17] in terms of the average DOS,  $\tilde{N}(M)$ , defined as  $M/(\mu_B H_{xc})$ , where  $(\mu_B H_{xc})$  is the (rigid) exchange splitting producing magnetic moment  $M$ :  $\Delta E = \int_0^M M dM / 2\tilde{N}(M)$ . The best visualization of the ESM is via plotting  $\tilde{N}(M)$  as a function of  $M$ . Wherever this curve crosses the line  $1/I$ , one has an extremum of the total energy. If the slope of the curve is positive at the intersection point, the extremum is a maximum, and the state is unstable, otherwise it is a minimum and indicates a (meta)stable magnetic state. The ESM plot for  $\text{CoS}_2$ , based on the LAPW DOS (Fig.2) is shown on Fig.3. At normal pressure, there are potentially two metastable states: a low spin, of the order of  $0.3 \mu_B$ , and a high spin, of the order of  $0.85 \mu_B$ . For Stoner parameter  $I < 0.63$  eV neither state is (meta)stable, for  $0.63 < I < 0.71$  eV only the low-spin state is, for  $0.70 < I < 0.73$  eV there are two metastable states, and for yet larger  $I$  only the high spin state may be realized. For  $I > 0.77$  eV ESM produces a HM. One can estimate  $I$  for a compound using the procedure described in Ref. [18], or deduce it by comparing the

ESM to fixed moment calculations. The latter method leads to  $I = 0.68$  eV for LMTO and  $I = 0.72$  eV for full potential calculations. The complicated structure of  $\tilde{N}(M)$  can be traced down to the structure of DOS near the Fermi level (Fig.2): after the initial drop of  $\tilde{N}(M)$ , it starts to increase again when the initially fully occupied peak at  $E - E_F \approx -0.1$  eV becomes magnetically polarized. The high-spin solution corresponds to the situation where this peak is fully polarized.

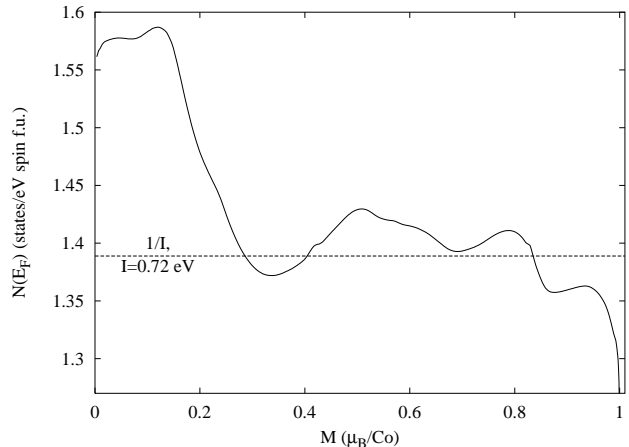


FIG. 3. Extended Stoner plot for  $\text{CoS}_2$ , showing the effective (averaged) density of states  $\tilde{N}(E_F)$  as a function of magnetic moment  $M$ . The horizontal line corresponds to a Stoner factor  $I = 0.72$  eV. The two crossing points near  $M \approx 0.3 \mu_B$ , and  $M \approx 0.8 \mu_B$ , show two (meta)stable states in the rigid band approximation.

Let me now consider the effect of pressure. Roughly speaking, applying pressure amounts to rescaling the band structure proportionally to squared inverse lattice parameter. Correspondingly, the density of states is rescaled proportional to  $(V_0/V)^{2/3}$ . The total energy in the ESM will include that as

$$E(V, M) \approx E_0 + \left(\frac{V}{V_0}\right)^{2/3} \int_0^M \frac{M dM}{2\tilde{N}(M, V_0)} - \frac{IM^2}{4} + \frac{B(V - V_0)^2}{2V_0}, \quad (1)$$

where  $V_0$ ,  $E_0$ , and  $B$  are the equilibrium volume, energy, and the bulk modulus, respectively, of the paramagnetic phase. The magnetic energy shifts the energy minimum towards larger volumes, a standard magnetostriction effect. What is unusual about the equation of states (1) with  $\tilde{N}(M, V_0)$  from Fig.3 is that for some range of values of  $I$  there are two local minima, a high spin state with a larger volume, and a low spin state with a smaller volume. The actual  $I$  seems to fall into this range. This suggests a first order phase transition with pressure, and there are indications [19] that it has been observed in the experiment [8], although the low spin state, which has  $M \approx 0.2 \mu_B$  in ESM and  $\approx 0.1 \mu_B$  in fixed mo-

ment calculations, was reported in Ref. [8] to have no or very small magnetic moment. Another consequence of the physical picture outlined here is metamagnetism: In the low spin state close to the critical pressure the system can be switched over to the high-spin state by an external magnetic field defined by the energy and magnetic moment difference between the two states. Again, metamagnetic behavior has been observed in  $\text{Co}(\text{S,Se})_2$ , in  $\text{Co}_{1-x}\text{Ni}_x\text{S}_2$ , and in compressed  $\text{CoS}_2$ . Finally, the theory predicts rapid increase of the equilibrium magnetization with *negative* pressure: in the ESM an expansion of 3-4% in volume already increases  $M$  to nearly  $1 \mu_B$ . This suggests that the spin fluctuations at high temperature (above  $T_C$ ) may have larger amplitude than the ordered moments at zero temperature. This kind of behavior has also been observed [20], and discussed in the literature [21].

The family of pyrite materials formed by 3d transition metals and chalcogens is incredibly rich. It shows various kinds of magnetism and metamagnetism, metal-insulator transitions of different types, superconductivity, and half metallicity. Except for the vicinity of a Mott-Hubbard transition, that is, close to  $\text{NiS}_2$ , the physics of these materials can be rather well understood within the local spin density functional theory. In particular, the extended Stoner formalism provides considerable insight into the magnetic behavior of this system. The most important conclusions from the calculations are:

1. The  $\text{Fe}_{1-x}\text{Co}_x\text{S}_2$  alloy is predicted to be a half metal in a large range of concentration. Unlike most other known half metals, and very importantly for the applications, the half-metallicity should be robust with respect to defects and crystallographic disorder.

2.  $\text{CoS}_2$  is an itinerant ferromagnet which has, due to a complicated structure of its density of states, two magnetic states: a high-spin one, with the moment  $M \sim 0.8 \mu_B$ , and a low-spin one, with  $M \lesssim 0.1 \mu_B$ . The first order transition to the low spin state can be induced by external pressure, doping with Se, or with Ni. In the low spin state the material exhibits metamagnetic properties. The structure of the density of states also manifests itself via an unusual temperature dependence of the magnitude of magnetic fluctuations.

3. The closeness of  $\text{CoS}_2$  to a magnetic phase transition also leads to strong coupling between electronic, lattice, and magnetic degrees of freedom, making it a relative of such "bad metals" as  $\text{SrRuO}_3$  and magnetoresistive manganites. Therefore interesting transport properties are to be expected in the system at and near stoichiometric composition, including large magnetoresistance and violation of the Yoffe-Regel limit at high temperatures.

For such an interesting, the 3d pyrites seem to be unusually little studied either experimentally or theoretically. Hopefully this paper will encourage further investigations.

- 
- [1] G.A. Prinz, *Science*, **282**, 1660 (1998).
  - [2] R. J. Soulen et al, *Science* **282**, 85 (1998).
  - [3] D. Orgassa *et al*, *Phys. Rev.***B 60** 13237 (1999).
  - [4] Here and below I speak about  $x > 1$ , meaning  $\text{CoS}_2$  doped with Ni instead of Fe.
  - [5] V. Eyert, K.H. Hock, S. Fiechter, and H. Tributsch, *Phys. Rev.***B 57**, 6350 (1998).
  - [6] Opahle I, Koepernik K, Eschrig H, *Phys. Rev.***B60**, 14035 (1999), and references therein.
  - [7] H.S. Jarret et al, *Phys. Rev. Lett.*, **21**, 617 (1968).
  - [8] T. Goto et al, *Phys. Rev.* **B56**, 14019 (1997).
  - [9] G. L. Krasko, *Phys. Rev. B* **36**, 8565 (1987); O.K. Andersen *et al*, *Physica* **86-88B**, 249 (1977).
  - [10]  $\text{CuS}_2$  has considerable density of states at the Fermi level, 1 st./eV spin f.u., and substantial electron-phonon interaction with high-frequency  $\text{S}_2$  vibrons. Our calculations for  $\text{CuS}_2$  will be published elsewhere. Note also that a very large electronic specific heat coefficient of 19.5 mJ/mole  $\text{K}^2$  was reported (S. Waki and S. Ogawa, *J. Phys. Soc. Jap.* **32**, 284, 1972), corresponding to a renormalization  $(1+\lambda) \approx 3$ . Of course, part of this renormalization should be coming from electron-magnon interaction, similar to, say,  $\text{SrRuO}_3$  [18].
  - [11] The Stuttgart package LMTO-TB 4.7 (<http://www.mpi-stuttgart.mpg.de/ANDERSEN/LMTODOC/LMTODOC.html>) was employed. Six automatically generated empty spheres were used per formula unit, and the result agreed reasonably well with the full-potential calculations (better than the alternative setup recommended in Ref. [5]) Somewhat unusual, the visual agreement between the band dispersions in LAPW and in LMTO is rather good, while the calculated magnetic moments differ by more than 20% ( $0.65 \mu_B$  in LMTO *vs.*  $0.85 \mu_B$  in LAPW). This is another indication that, as discussed below in the text, the stoichiometric system is close to a high spin – low spin transition.
  - [12] The WIEN-97 package was used (P. Blaha, K. Schwarz, and J. Luitz, Vienna University of Technology, 1997, improved and updated version of the code published by P. Blaha *et al*, *Comp. Phys. Commun.*, **59**, 399, 1990).
  - [13] I.I. Mazin, to be published elsewhere.
  - [14] Noticeable magnetization of S has been confirmed experimentally (A. Ohsawa *et al*, *J. Phys. Soc. Jap.* **40**, 992, 1976).
  - [15] Regarding calculations of the Stoner factor  $I$  for compounds, the reader is referred, for instance, to Ref. [18]
  - [16] H. Yamada, K. Terao, and M. Aoki, *J. Mag. Mag. Mater.* **177**, 607 (1998).
  - [17] This formula follows from the fact the derivative of the one-electron energy with respect to  $M$  is  $(\mu_B H_{xc})/2 = (M/2)/\tilde{N}(M)$ .
  - [18] I.I. Mazin and D.J. Singh, *Phys. Rev.* **B56**, 2556 (1997).
  - [19] Experimentally, the transition at the Curie temperature becomes first order at  $P \gtrsim 0.4$  GPa.
  - [20] N. Inoue and H. Yasuoka, *Sol. State Comm.* **30**, 341 (1979).
  - [21] S. Ogawa, *J. Mag. Mag. Mater.* **31-34**, 269 (1983).